COMPDYN 2019
7th ECCOMAS Thematic Conference on
Computational Methods in Structural Dynamics and Earthquake Engineering
M. Papadrakakis, M. Fragiadakis (eds.)
Crete, Greece, 24–26 June 2019

ON THE EFFICIENT RISK ASSESSMENT OF BRIDGE STRUCTURES

Gerard J. O'Reilly[1] **and Ricardo Monteiro**[2]

[1] Scuola Universitaria Superiore IUSS Pavia
Palazzo del Broletto, Piazza della Vittoria 15, Pavia 27100, Italy
e-mail: gerard.oreilly@iusspavia.it

[2] Scuola Universitaria Superiore IUSS Pavia
Palazzo del Broletto, Piazza della Vittoria 15, Pavia 27100, Italy
email: ricardo.monteiro@iusspavia.it

Abstract

In performance-based seismic assessment, structural response is characterised with increasing seismic intensity via some form of intensity measure (IM). IMs are typically related to the characteristics of ground shaking and dynamic properties of the structure, with spectral acceleration at the first and dominant mode of vibration being a popular choice in the case of buildings. In bridge structures, where no single dominant mode typically exists for bridges with any degree of irregularity, the use of spectral acceleration at one single mode of vibration may be somewhat inefficient due to a more multi-modal transverse structural response. To counter this and also to appease the needs of bridge portfolio assessment, where a group of structures is assessed collectively to evaluate entire bridge networks, peak ground acceleration has become a popular IM, albeit its drawbacks in terms of meaning with respect to structural dynamics. To address these limitations, this paper explores the use of different IMs for a more efficient assessment of bridges. Among these, there is average spectral acceleration, whereby a pertinent period range is used to define the IM that could suit the needs of a bridge structure with multi-modal response as well as when more than one bridge structure is considered. To do this, a number of bridges are considered and evaluated via incremental dynamic analysis for different IMs. The results show that average spectral acceleration is indeed a quite efficient IM that can lead to a more refined quantification of bridge performance, both individually and also as part of a larger bridge network when conducting portfolio risk assessment.

Keywords: bridges; assessment; intensity measure; average spectral acceleration; portfolio.

1 INTRODUCTION

One aspect that is required in the site-specific seismic hazard assessment of a structure is the choice of an intensity measure (IM), that is, the measure used to characterise the intensity of ground shaking to be linked to different levels of damage when deriving fragility curves. Different types of IMs exist, with each one possessing their own inherent advantages and disadvantages [1–5]. One aspect that is typically desirable from any IM is for it to be efficient, meaning that is should be a relatively accurate predictor of the structural response and subsequently, the damage. This characteristic typically leads IMs to be defined in terms of the modal properties of the structure, with the first mode spectral acceleration, $Sa(T_1)$, being a popular choice in building assessment, since the response of the building is generally dominated by the first mode response. Ground motion records can subsequently be selected and conditioned to that specific period using conventional tools (e.g. conditional spectrum [6–8]) and the numerical analysis subsequently conducted.

In the case of bridges, there does not generally tend to be a dominant mode of transverse response (i.e. a mode of response where most of the mass is participating), which therefore makes the task of choosing a single period to characterise the IM in terms of $Sa(T)$ more difficult. Furthermore, when dealing with the assessment of large numbers of bridges as part of a regional or portfolio assessment, it is almost certain that each bridge will possess different first mode of vibration periods, making the IM choice even more taxing. This is because a single period may be efficient for some types of bridges while not for others, resulting in increased dispersion and reduced IM efficiency. To avoid this issue in regional assessment, peak ground acceleration (PGA) has often been adopted in the past [9]. While this is a simple and convenient solution, PGA is widely known to be a relatively poor predictor of structural response but has been shown [10] to be a fair performer for bridges when compared to other types of IMs, therefore still having some merit.

A further aspect regarding IM definition is that it requires some knowledge of the structure's modal properties, which are often not known prior to construction of the numerical models. Hence, the adoption of an IM that does not require modal properties is preferred. One candidate that has emerged as a potential solution to the aforementioned problems is average spectral acceleration, *AvgSa*, defined as the geometric mean of *N*-number spectral accelerations within a user-specified range [T_{lower}, T_{upper}] as described by Equation (1):

$$AvgSa = \left[\prod_{i=1}^{N} Sa(T_i)\right]^{1/N} \quad for\ T \in [T_{lower}, T_{upper}] \tag{1}$$

This has the benefit of being relatively simple in its definition and being relatively independent of modal properties. When compared to the efficiency of other more building-specific IMs like $Sa(T_1)$, studies [11,12] have shown *AvgSa* to perhaps not be the outright winner in any specific category of response prediction (e.g. storey drift, floor acceleration or collapse performance) but to be the best across the board when considering all salient structural response parameters. It works on the basis of defining a period range of interest over which the hazard is conditioned, instead of a specific period. As such, the precise value of a structure's period(s) is not required (as for $Sa(T_1)$) but rather a range in which they are likely to fall. This is advantageous when assessing multiple structures since the modal properties of a single structure are not focused on and an acceptable level of efficiency is still being maintained. For bridge structures, where there is usually no single dominant mode of vibration, the use of a period range also makes more sense since the entire response cannot be adequately linked to a single mode of vibration as in the case of buildings.

This study examines the efficiency of different IMs for the assessment of bridges structures, particularly *AvgSa*. It builds on past work by Zelaschi *et al.* [5] and Monteiro *et al.* [10] by assessing the relative IM efficiency for a number of regular and irregular structures via incremental dynamic analysis (IDA) [13]. The level of damage is assessed via local member-specific parameters and the evolution of pier damage in the bridge is characterised with increasing intensity. A number of IMs are considered using these analysis results, relative comparisons are made and conclusions are drawn.

2 CASE STUDY

2.1 Description of bridge structures

To examine the impact of using different IMs for fragility assessment, a number of case study bridge structures were examined. These structures were previously examined by Pinho *et al.* [14] to evaluate different non-linear static analysis procedures for bridge structures. The case study comprised bridge structures of two lengths, with viaducts consisting of either four or eight 50m spans. Bridges were classed as being regular or semi-irregular/irregular depending on the variations of bridge pier heights considered, which are illustrated in Figure 1. For each pier, the same cross section was assumed, whose details are given in Figure 2. This way, different bridge pier configurations – and therefore distributions of bridge pier stiffness and subsequent mode shapes – could be examined in a relatively simple manner, whilst at the same time maintaining a degree of realism for what concerns the general irregularity of bridges. The total number of bridges was seven, as implied by Figure 1, where the label numbers 1, 2, and 3 denote pier heights of 7m, 14m, and 21m, respectively.

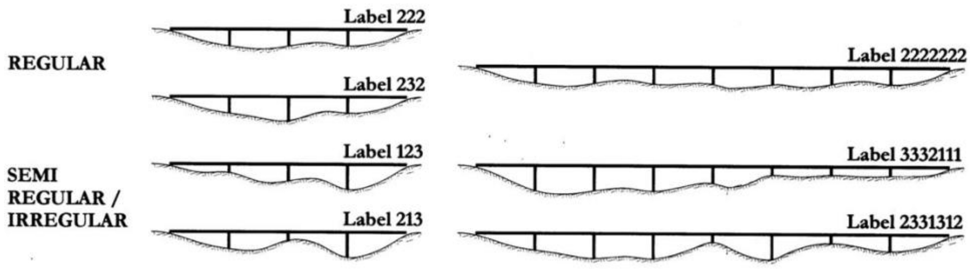

Figure 1. Illustration of the longitudinal profile of the bridge structures considered, where the different labels refer to the arrangement of pier heights in multiples of 7m.

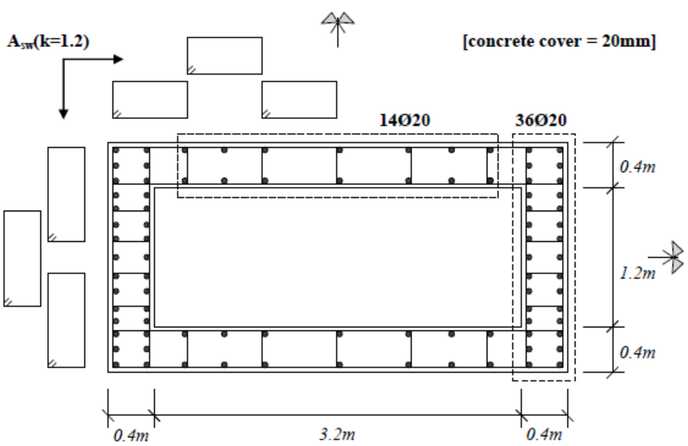

Figure 2. Details of the cross section utilised for each bridge pier [14], where the shorter side of the section is placed in the direction of the bridge deck.

2.2 Numerical modelling of bridge

A numerical model of each bridge was built using OpenSees [15]. The dimensions of the bridge structures are as per Figure 1, with each pier cross section comprising the section dimensions and reinforcement layout illustrated in Figure 2. The piers were modelled as fixed at the base and the deck ends were supported upon pot bearings with a horizontal stiffness of 26,329 kN/m. The deck system was modelled using a continuous elastic beam-column element whose section stiffness properties were modelled as reported by Pinho *et al.* [14].

Pier elements were modelled using lumped plasticity elements, whose parameters were established from moment-curvature analysis. To do this, the Concrete01 material model available in OpenSees was used. The characteristic compressive strength of concrete was taken as 42MPa and the strain at peak stress was taken to be 0.002. Based on the layout of the concrete shear reinforcement in Figure 2, the confinement factor was computed as 1.2 and its impact on the stress-strain relationship for the confined regions of the pier cross-section was incorporated as per Mander *et al.* [16]. As such, cover concrete was modelled as unconfined, whereas the inner regions restrained by the stirrups were modelled as confined. Reinforcing steel was modelled using the Steel02 material model in OpenSees with a yield strength of 500MPa. To simulate the rupture of the bars, a MinMax criterion was placed on this material to simulate its loss of strength when a certain strain threshold was surpassed. This rupture strain was estimated as 0.10 based on the values given in Priestley *et al.* [17] for reinforcement steel used in bridges in Europe. Since three types of pier element were feasible (i.e. 7m, 14m or 21m), moment-curvature was conducted for each axial load ratio resulting from the change in pier self-weight. Once established, the Pinching4 material model was used to capture the moment-curvature behaviour shown in Figure 3 and used in the lumped plasticity element model.

All elements were modelled using the corotational geometric transformation to model second-order effects. Masses were modelled as distributed along both the deck and the pier elements. Priestley *et al.* [17] suggested that simply placing one-third of the pier mass at its top as a lumped mass may also suffice, which would result in a more efficient numerical model. However, this simplification assumes the formation of a plastic mechanism at the base and a linear displaced shape along the pier height, which would be difficult to justify for some of the more irregular configurations shown in Figure 1. Gravity loads were also applied and maintained throughout all analyses.

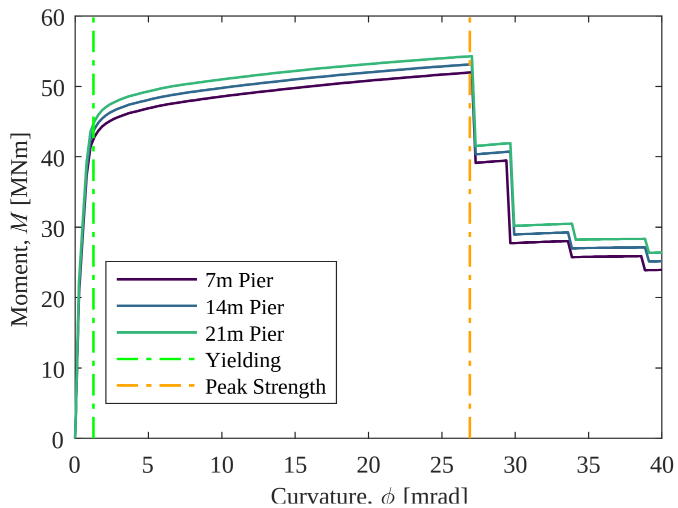

Figure 3. Characterisation of each pier element's moment-curvature behaviour and definition of the two limit states corresponding to section yielding and peak strength prior to the initiation of bar rupture.

3 RESPONSE CHARACTERISATION

3.1 Modal analysis

With a numerical model of each bridge structure constructed, the next step was to conduct a modal analysis and identify their dynamic properties. Table 1 presents the periods for the first three modes of vibration in the transverse direction of response. It can be seen that some of the periods tend to be closely spaced with none of the modes comprising the majority of the modal mass. This confirms how, unlike building structures, there tends not to be a predominant mode of response that can be used to characterise the entire structural response. It is also worth noting how the first three modes of the more regular bridge structures comprise most of the mass, whereas for the irregular cases there is an overall poor representation of modal mass.

Table 1. Modal properties of each bridge numerical models, where periods of vibration and percentage modal mass for the first three modes in addition to their sum are shown.

Bridge	Configuration	Type	T_1 [s]	T_2 [s]	T_3 [s]	$\%M_1$	$\%M_2$	$\%M_3$	Sum $\%M$
1	123	Irregular	0.5550	0.4470	0.2770	28	9	12	48
2	213	Irregular	0.5550	0.4740	0.2530	27	17	1	45
3	222	Regular	0.4830	0.4750	0.2230	31	0	57	88
4	232	Regular	0.5080	0.4750	0.3070	19	0	76	95
5	2222222	Regular	0.4790	0.4790	0.2250	16	0	74	89
6	2331312	Irregular	0.4940	0.4740	0.3600	4	9	29	42
7	3332111	Irregular	0.5560	0.4360	0.3870	11	7	29	47

3.2 Incremental dynamic analysis

IDA was performed to characterise the response of the bridge structures with increasing ground motion intensity using the far-field ground motion set from the FEMA P-695 guidelines [18]. Analyses were conducted in the transverse direction and a 2% tangent stiffness-proportional Rayleigh damping model was adopted. This was based on past experimental observations [19] because in the case of bridge structures, the lack of contribution to the energy dissipation typically provided by damage to non-structural elements in buildings, amongst other sources, is not present.

To characterise the bridge response with increasing intensity, a single structural demand parameter - termed an *engineering demand parameter* (EDP) - was needed. In buildings, roof drift ratio or maximum storey drift along the building height are typical EDPs, since they characterise the response of these first mode dominated structures quite well. Again, in the case of bridges, the lack of a dominant mode or an obvious critical element in the structure makes the identification of a suitable EDP a non-trivial task. Global EDPs, such as peak deck displacement, may be used but these do not necessarily differentiate the degree of inelastic damage in piers of different height. As such, local element-oriented EDPs were sought here. Monteiro *et al.* [10] followed the work of Nielson [20] and HAZUS [21] by utilising the maximum displacement-based ductility of all piers as their EDP. A similar approach was adopted here: the peak transient curvature at the base of the piers was monitored during ground shaking to obtain the peak pier section curvature. The maximum value of peak pier section curvature among all piers of the bridge, φ_{max}, was then identified as the EDP.

Two limit states were identified, corresponding to pier section yielding and the peak strength, beyond which the section begins to lose its capacity due to rupturing of the reinforcement bars. The yield curvature was computed from Priestley *et al.* [22] and for peak strength, the section curvature was computed via the reinforcement rupture strain limit previously described in Section 2.2. Both limit state definitions were considered independent of pier height and therefore a single set was used throughout, as illustrated in Figure 3. These two limit states – termed *yielding* and *peak strength* herein – correspond to 1.25mrad and 26.9mrad, respectively, implying a curvature-based ductility capacity of approximately 21.5 in the bridge piers.

3.3 Intensity measure definition

To characterise the evolution of structural damage using IDA, an IM definition was required. Since the purpose of this study was purely to evaluate the relative efficiency of different IMs in their ability to characterise bridge response, numerous IMs were considered. This was because different IMs could be defined using the same set of IDA results via a simple re-processing. For example, for a single bridge model whose response to a given ground motion signal is a known value via non-linear dynamic analysis, its intensity can be examined in numerous ways (e.g. peak ground acceleration or spectral acceleration at a given period). IM is an interface variable used to quantify a ground motion's shaking intensity with respect to structural EDP. Therefore, for a given ground motion signal, or set of signals in this study's case, any number of IMs may be examined.

As such, the IDA was conducted using *PGA* as the initial reference IM with a number of alternative IMs considered via re-processing of the IDA results. The IMs considered as part of this study were:

- *PGA* – defined as the peak ground acceleration of a given ground motion;
- $Sa(T_1)$ – the 2%-damped spectral acceleration at the first mode period, T_1, for a given bridge structure;
- $Sa(T_{med})$ – the 2%-damped spectral acceleration at the median period of the first three modes, $T_1 - T_3$, for the bridges listed in Table 1;
- *PGV* – defined as the peak ground velocity of a given record;
- *AvgSa* – the average spectral acceleration defined in Equation (1) as the geometric mean of ten equally space periods spanning the range of T_{lower} and T_{upper} defined below.

In the case of *PGA* and *PGV*, these quantities are self-explanatory and are simply defined as the absolute peak of the ground acceleration and velocity of each individual accelerogram, meaning that they were not in any way connected to the bridge dynamic properties. On the other hand, $Sa(T_1)$ and $Sa(T_{med})$ correspond to the spectral accelerations at specified periods of the bridges or bridge groups, meaning that some period information was required for their definition.

For *AvgSa*, a period range [T_{lower}, T_{upper}] needed to be defined. It did not need to be linked to any bridge period in particular but rather ensure sufficient coverage of the period range of interest. To define this range, the modal properties listed in Table 1 were used. Considering these modal properties, a period range spanning T_{lower}=0.112s and T_{upper}=0.833s was established for the case study bridges. T_{lower} was determined as 0.5 times the 16th percentile of the T_3 values whereas T_{upper} was determined as 1.5 times the 84th percentile of the T_1 values. The lower limit was defined as the 16th percentile value in order to cover the majority of the higher mode values and not be biased by any outlier period value. It was further factored down by 0.5 to anticipate other modal contributions since Table 1 indicated that the irregular bridge configurations tended to have many different modes beyond the third contributing to the dynamic response. The upper limit was established using the 84th percentile to cover the majority of the first mode periods and amplified by 1.5 to account for the effects of period elongation during non-linear response. A range of ten periods equally spanning this range was used to define *AvgSa*. In the absence of actual modal information for bridge groups, simple empirical relationships [23] may also be used to identify the likely ranges in which T_{lower} and T_{upper} should be defined.

4 RESULTS

Conducting IDA for each bridge structure, their response was characterised well into the non-linear range of response. Each of the five aforementioned IMs were subsequently used to describe and examine the bridge response. Figure 4 illustrates the response of Bridge 2 for the $Sa(T_1)$ and *AvgSa* IMs, for example, where the two limit states defined in Figure 3 are also highlighted. The exceedance of these limit states was assumed to adequately characterised by a lognormal distribution, whose dispersion is defined as the standard deviation of the natural logarithm of the data. Considering the intersection of these vertical lines characterising the two limit states, the dispersion due to record-to-record variability, β_{RTR}, of each IM could examined and characterised. Figure 5 illustrates the dispersions of each IM at both limit states for all seven bridge structures examined. Tentatively operating on the premise that lower dispersion implies a better or more accurate quantification of response and, in turn, risk, some initial observations can be made.

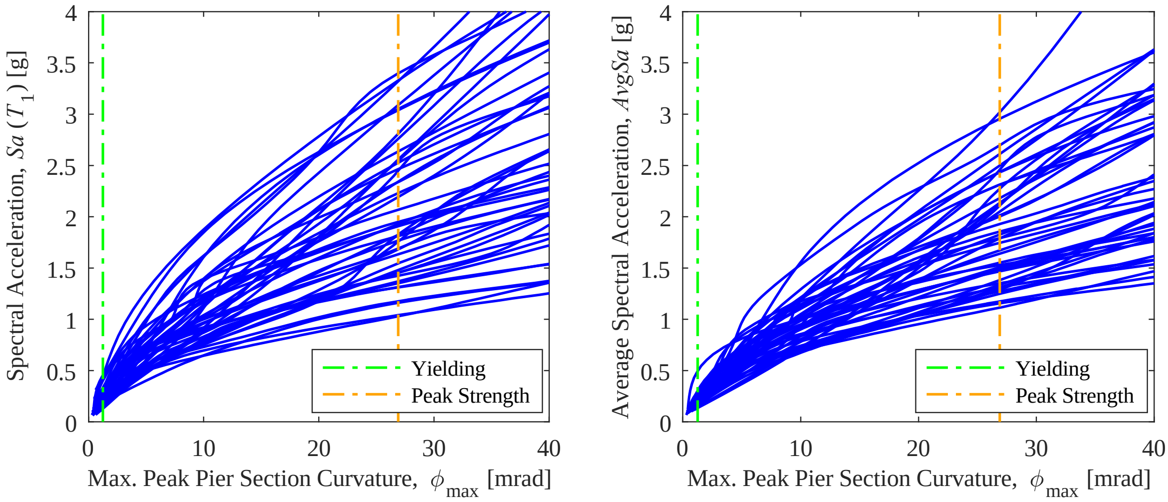

(a) $Sa(T_1)$ (b) *AvgSa*

Figure 4. Illustration of the IDA results obtained for Bridge when plotted for different IMs.

From Figure 5, *PGA*, $Sa(T_1)$ and $Sa(T_{med})$ are seen to be fair indicators of structural response at both limit states. At yielding, they all tend to produce the same level of dispersion, whereas for the peak strength limit state, *PGA* tended to produce slightly lower dispersion on average. This indicates that there is no clear advantage to using mode-specific IMs for bridge structures since the lack of a dominant mode makes one spectral definition as valid as another, roughly speaking. It was also interesting to note the general inefficiency of the $Sa(T)$-based IMs for regular bridges (i.e. Bridges 3, 4 and 5) at the peak strength limit state. This was a rather unusual observation at first but upon further inspection of the modal masses in Table 1, it can be seen how the more dominant modes for these bridges were in fact the third modes of response and not the first. Careful consideration of the modal properties could have reduced this dispersion by using $Sa(T_3)$ but it actually goes to show how further considerations are required to use such IMs for bridges. Overall, it appears that the *PGV* and *AvgSa* IMs were the best performers as they rendered the lower dispersions on average. *PGV* slightly outperforms *AvgSa* at the peak strength limit state, which resonates the findings of Monteiro *et al.* [10], but it is seen to report very high levels of dispersions at the yielding limit state. On the other hand, *AvgSa* was seen to have the lowest dispersion for most cases at both limit states. This finding also goes along with the conclusions of Kohrangi *et al.* [11] when using *AvgSa* for assessing existing buildings, stating that *AvgSa* may not be the best performer in any one single category but tends to be the best overall IM to characterise different facets of structural performance.

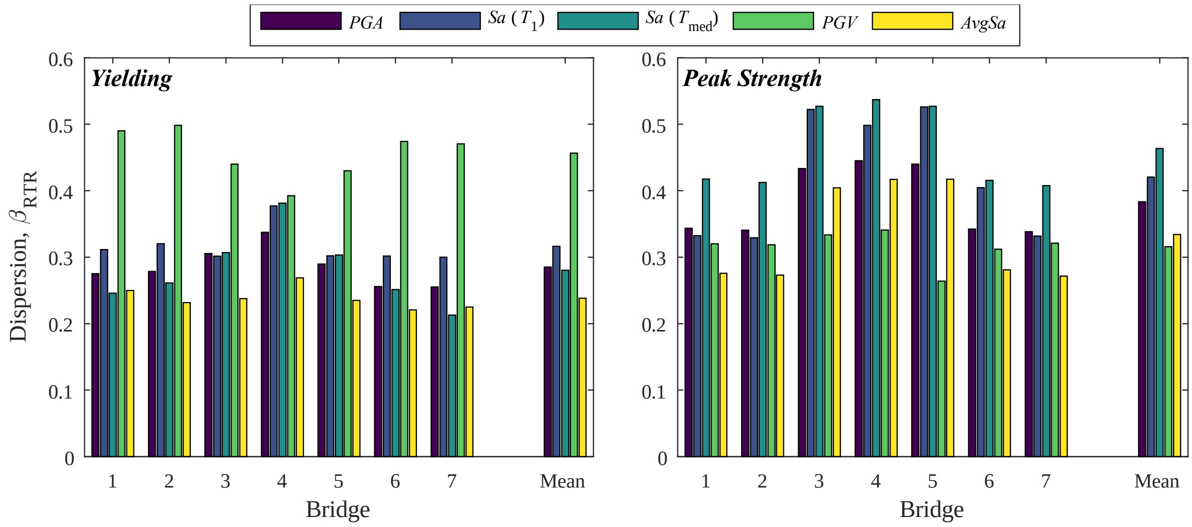

Figure 5. Relative comparison of the dispersions for each bridge structure for both yield and peak strength limit states along with mean dispersion for the bridge group.

While the above comparison in terms of dispersion for different IMs is useful to gauge the general IM efficiency, no definitive conclusions may be drawn in terms of the 'best' IM since the dispersion in the respective ground motion prediction equations (GMPEs) must also be considered. That is, a very complex and detailed IM may be defined to optimise and report very low levels of dispersion for the structural response, but the level of uncertainty with its associated GMPE may be very large, meaning that the uncertainty has simply been moved from one part of risk assessment to another, since risk is quantified via the integration of hazard and vulnerability. The above comparison and comments relating to Figure 5 will only hold true if the GMPE uncertainty of the IMs remains similar. As such, a brief comparison of the dispersion associated with the GMPEs is included here to support the general findings of this study.

For the IMs defined using spectral values or general characteristics of the ground motion shaking (i.e. *Sa*(*T*), *PGA* and *PGV*) the IM dispersion, β_{IM}, is typically provided as a GMPE output for a given rupture scenario. For instance, GMPEs such as Campbell and Bozorgnia [24] provide it for each of the IMs listed previously. In the case of *AvgSa*, however, some further consideration is required since it is an IM made up of a combination of other IMs (i.e. the geometric mean of *Sa*(*T*) values). *AvgSa* dispersion for a given rupture scenario, $\beta_{\mathrm{AvgSa|rup}}$, has been shown [11,25] to be described according to Equation (2):

$$\beta^2_{AvgSa|rup} = \left(\frac{1}{N}\right)^2 \sum_{i=1}^{N} \sum_{j=1}^{N} \rho_{\ln Sa(T_{\mathrm{i}}),\, \ln Sa(T_{\mathrm{j}})} \sigma_{\ln Sa(T_{\mathrm{i}})|rup} \sigma_{\ln Sa(T_{\mathrm{j}})|rup} \tag{2}$$

where N is the number of spectral values being averaged (10 in this study), σ represents the *Sa*(*T*) dispersion for a given rupture scenario provided by GMPEs, and ρ represents the correlation between the spectral values at two periods, T_{i} and T_{j}, which can be computed using a model such as that by Baker and Jayaram [26].

To illustrate the difference in relative GMPE dispersions between the IMs considered in Figure 5 and shed more light on the efficiency of these IMs, a rupture scenario was considered. Figure 6 shows the IM dispersions computed using the aforementioned GMPEs for a rupture scenario of magnitude 7.0, at a distance of 50km and on soil with V_{s30}=360m/s, corresponding to firm ground. Overall, it can be seen from Figure 6 how the relative dispersions of the different IMs are relatively similar, with no single one having a markedly higher or lower dispersion than another. What is important to note is that, of the favourable IMs in Figure 5, there is no significant disadvantage to their use also from a GMPE dispersion point of view. *PGA* and *PGV* are seen to have slightly lower dispersion with respect to the $Sa(T)$-oriented counterparts. This goes to show how the poor predictability of structural response by these $Sa(T)$-oriented IMs (i.e. β_{RTR}) only gets exacerbated by the relatively high variability in the GMPE. Compared to *AvgSa* at both limit states and *PGV* at the peak strength limit state, where the dispersion in structural response and in the GMPE are lower, this indicates an overall better IM performance. This lower GMPE dispersion was noted by Kohrangi *et al.* [11] to be a characteristic of *AvgSa*'s definition. With respect to the $Sa(T)$-oriented IMs, *PGA* is seen not to be a bad option, a finding also noted by Monteiro *et al.* [10], but when compared to *PGV* and *AvgSa*, is seen to be slightly inferior in terms of efficiency. Of course, these conclusions are based on visual inspection of few case studies and more thorough studies ought to be used in order to provide more definitive conclusions. Nevertheless, it provides useful insight into the efficiency of different IMs and their usability in the specific case of bridge structures, where many different dynamic properties often taken for granted in the case for buildings do not necessarily apply.

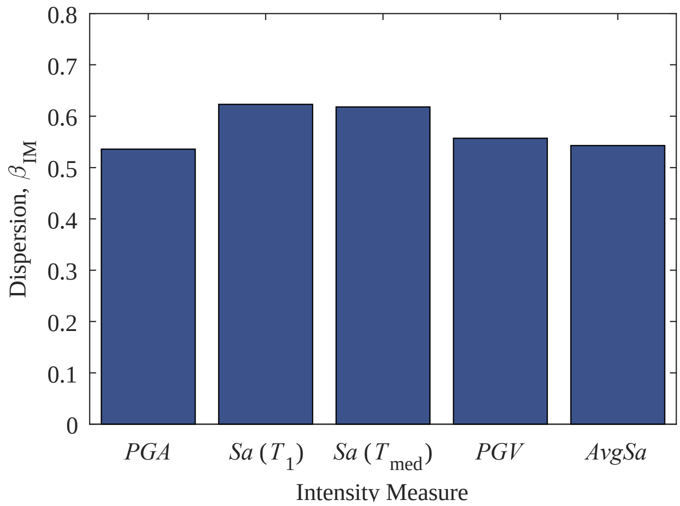

Figure 6. Comparison of the GMPE dispersion associated with each IM.

5 SUMMARY AND CONCLUSIONS

This work examined the relative performance of different intensity measures (IM) for the assessment of bridge structures. To do this, a number of bridges, both of regular and irregular configuration, were modelled and analysed. Their dynamic response with respect to increasing ground shaking intensity was characterised and the exceedance of two limit states corresponding to pier section yielding and peak strength were quantified. A number of IMs were used to examine how efficiently each could characterise the bridge response at both limit states. IMs related to ground motion parameters such as peak ground acceleration (*PGA*) and peak ground velocity (*PGV*), in addition to others related to the bridge structures' modal properties like spectral acceleration, $Sa(T)$, were examined. Furthermore, a recently introduced IM termed average spectral acceleration, *AvgSa*, was also examined. Their efficiency was evaluated in terms of dispersion for each limit state. The results showed that the level of dispersion depended on the type of IM, the regularity of the bridge structures and the limit state being considered. Based on this preliminary study, the following conclusions can be noted:

- Due to the inherent nature of their dynamic properties, bridge structures are generally not characterised by a single dominant period of response, with numerous modes of response contributing depending on the bridge layout’s regularity. This can make *Sa*(*T*)-oriented IMs rather unfavourable;
- *PGA* and *PGV* tend to be better predictors of structural response when compared to the first mode spectral acceleration, $Sa(T_1)$, as their dispersion was generally lower;
- Considering the median period value of the bridge group’s first three periods in a *Sa*(*T*)-oriented IM did not offer much improvement in terms of IM efficiency;
- *PGV* was seen to be one of the best predictors of bridge response for the peak strength limit state, which signifies extensive pier damage, but was noted to be one of the worst predictors of the low damage limit state related to pier section yielding;
- Overall, *AvgSa* was seen to be the best predictor of bridge response. This was the case for both limit states and bridge configurations;
- In terms of GMPE dispersion, the increased dispersion of the *Sa*(*T*)-oriented IMs saw their overall efficiency further exacerbated for risk assessment of bridges, while *AvgSa* was shown to be slightly superior to *PGA* and *PGV* in this sense.

While the study presented here represents a relatively simple illustration of the potential benefits of using IMs such as PGV or AvgSa that are relatively independent of the bridge dynamic properties, further work is required to verify the observations made. Nevertheless, these findings are promising for what concerns the risk assessment of bridge structure groups as part of regional or portfolio assessment.

6 ACKNOWLEDGEMENTS

The authors would like to acknowledge the financial support of the INFRA-NAT project (www.infra-nat.eu) co-funded by European Commission DG-ECHO – Humanitarian Aid and Civil Protection. Project reference: 783298 – INFRA-NAT – UCPM-2017-PP-AG.

REFERENCES

[1] Eads L, Miranda E, Lignos DG. Average spectral acceleration as an intensity measure for collapse risk assessment. Earthq Eng Struct Dyn 2015;44:2057–73. doi:10.1002/eqe.2575.

[2] Kazantzi AK, Vamvatsikos D. Intensity measure selection for vulnerability studies of building classes. Earthq Eng Struct Dyn 2015;44:2677–94. doi:10.1002/eqe.2603.

[3] Kazantzi AK, Vamvatsikos D. A Next Generation Scalar Intensity Measure for Analytical Vulnerability Studies. COMPDYN 2015 - 5th ECCOMAS Themat. Conf. Comput. Methods Struct. Dyn. Earthq. Eng., Crete Island, Greece: 2015.

[4] Bradley BA. A generalized conditional intensity measure approach and holistic ground-motion selection. Earthq Eng Struct Dyn 2010;39:1321–42. doi:10.1002/eqe.995.

[5] Zelaschi C, Monteiro R, Pinho R. Critical Assessment of Intensity Measures for Seismic Response of Italian RC Bridge Portfolios. J Earthq Eng 2017:1–21. doi:10.1080/13632469.2017.1342293.

[6] Baker JW. Conditional Mean Spectrum: Tool for Ground-Motion Selection. J Struct Eng 2011;137:322–31. doi:10.1061/(ASCE)ST.1943-541X.0000215.

[7] Lin T, Haselton CB, Baker JW. Conditional spectrum-based ground motion selection. Part I: Hazard consistency for risk-based assessments. Earthq Eng Struct Dyn 2013;42:1847–65. doi:10.1002/eqe.2301.

[8] Lin T, Haselton CB, Baker JW. Conditional spectrum-based ground motion selection. Part II: Intensity-based assessments and evaluation of alternative target spectra. Earthq Eng Struct Dyn 2013;42:1867–84. doi:10.1002/eqe.2303.

[9] Borzi B, Ceresa P, Franchin P, Noto F, Calvi GM, Pinto PE. Seismic Vulnerability of the Italian Roadway Bridge Stock. Earthq Spectra 2015;31:2137–61. doi:10.1193/070413EQS190M.

[10] Monteiro R, Zelaschi C, Silva A, Pinho R. Derivation of Fragility Functions for Seismic Assessment of RC Bridge Portfolios Using Different Intensity Measures. J Earthq Eng 2017:1–17. doi:10.1080/13632469.2017.1387188.

[11] Kohrangi M, Bazzurro P, Vamvatsikos D, Spillatura A. Conditional spectrum-based ground motion record selection using average spectral acceleration. Earthq Eng Struct Dyn 2017. doi:10.1002/eqe.2876.

[12] O'Reilly GJ, Kohrangi M, Bazzurro P, Monteiro R. Intensity Measures for the Collapse Assessment of Infilled RC Frames. 16th Eur. Conf. Earthq. Eng., Thessaloniki, Greece: 2018.

[13] Vamvatsikos D, Cornell CA. Incremental dynamic analysis. Earthq Eng Struct Dyn 2002;31:491–514. doi:10.1002/eqe.141.

[14] Pinho R, Monteiro R, Casarotti C, Delgado R. Assessment of continuous span bridges through nonlinear static procedures. Earthq Spectra 2009;25:143–59. doi:10.1193/1.3050449.

[15] McKenna F, Scott MH, Fenves GL. Nonlinear Finite-Element Analysis Software Architecture Using Object Composition. J Comput Civ Eng 2010;24:95–107. doi:10.1061/(ASCE)CP.1943-5487.0000002.

[16] Mander JB, Priestley MJN, Park R. Theoretical Stress-Strain Model for Confined Concrete. J Struct Eng 1988;114:1804–26.

[17] Priestley MJN, Seible F, Calvi GM. Seismic Design and Retrofit of Bridges. John Wiley & Sons, Ltd.; 1996.

[18] FEMA P695. Quantification of Building Seismic Performance Factors. Washington, DC, USA: 2009.

[19] Correia AA, Almeida JP, Pinho R. Seismic energy dissipation in inelastic frames: Understanding state-of-the-practice damping models. Struct Eng Int J Int Assoc Bridg Struct Eng 2013;23:148–58. doi:10.2749/101686613X13439149157001.

[20] Nielson BG. Analytical fragility curves for highway bridges in moderate seismic zones. Georgia Institute of Technology, USA, 2005.

[21] HAZUS. Multi-Hazard Loss Estimation Methodology Earthquake Model. Washington, DC, USA: 2003.

[22] Priestley MJN, Calvi GM, Kowalsky MJ. Displacement Based Seismic Design of Structures. Pavia, Italy: IUSS Press; 2007.

[23] Zelaschi C, Monteiro R, Pinho R. Parametric Characterization of RC Bridges for Seismic Assessment Purposes. Structures 2016;7:14–24. doi:10.1016/j.istruc.2016.04.003.

[24] Campbell KW, Bozorgnia Y. NGA Ground Motion Model for the Geometric Mean Horizontal Component of PGA, PGV, PGD and 5% Damped Linear Elastic Response Spectra for Periods Ranging from 0.01 to 10 s. Earthq Spectra 2008;24:139–71. doi:10.1193/1.2857546.

[25] Dávalos H, Miranda E. A Ground Motion Prediction Model for Average Spectral Acceleration. J Earthq Eng 2018;00:1–24. doi:10.1080/13632469.2018.1518278.

[26] Baker JW, Jayaram N. Correlation of Spectral Acceleration Values from NGA Ground Motion Models. Earthq Spectra 2008;24:299–317. doi:10.1193/1.2857544.